Model Fe-Al Steel with Exceptional Resistance to High Temperature Coarsening. Part II: Experimental Validation and Applications

TIHE ZHOU, PENG ZHANG, RONALD J. O'MALLEY, HATEM S. ZUROB, and MANI SUBRAMANIAN

In order to achieve a fine uniform grain-size distribution using the process of thin slab casting and directing rolling (TSCDR), it is necessary to control the grain-size prior to the onset of thermomechanical processing. In the companion paper, *Model Fe-Al Steel with Exceptional Resistance to High Temperature Coarsening. Part I: Coarsening Mechanism and Particle Pinning Effects*, a new steel composition which uses a small volume fraction of austenite particles to pin the growth of delta-ferrite grains at high temperature was proposed and grain growth was studied in reheated samples. This paper will focus on the development of a simple laboratory-scale setup to simulate thin-slab casting of the newly developed steel and demonstrate the potential for grain size control under industrial conditions. Steel bars with different diameters are briefly dipped into the molten steel to create a shell of solidified material. These are then cooled down to room temperature at different cooling rates. During cooling, the austenite particles nucleate along the delta-ferrite grain boundaries and greatly retard grain growth. With decreasing temperature, more austenite particles precipitate, and grain growth can be completely arrested in the holding furnace. Additional applications of the model alloy are discussed including grain-size control in the heat affected zone in welds and grain-growth resistance at high temperature.

I. INTRODUCTION

THIN slab casting and directing rolling (TSCDR) has become a major process for hot strip production due to its low capital and operating costs.[1,2] For a typical compact strip production (CSP) mill, the molten steel is fed *via* the ladle and tundish into a funnel-shaped mold. Solidification starts on the mold wall and the external solidified shell increases in thickness as the steel strand transits the mold. Leaving the mold, the thin slab runs through to the secondary cooling zone and continues its solidification. It is cut to length by a pendulum shear and then sent to the soaking furnace. After descaling, the slab is rolled in the CSP hot strip mill; the resulting hot strip then goes through the laminar cooling system and is fully coiled.[3] Solidification of most microalloyed steels with carbon contents below 0.08 wt pct starts around 1798 K (1525 °C) as delta-ferrite and is completed at about 1770 K (1497 °C). When temperature drops below 1750 K (1477 °C), the delta-ferrite begins to transform to austenite. This phase transformation is completed at about 1721 K (1448 °C). The main microstructural event after the formation of austenite and prior to thermomechanical processing is austenite grain growth. The austenite grain growth could be divided into two regimes. The first regime corresponds to cooling from 1721 K to 1423 K (1448 °C to 1150 °C) before entering the soaking furnace. The second regime corresponds to isothermal holding within the soaking furnace, typically at 1473 K to 1373 K (1200 °C to 1100 °C) for a duration of 20 to 45 minutes. In the absence of particle pinning, the austenite grain size can increase from ~250 to about 2000 μm during the above cooling and isothermal holding steps.[4,5]

In order to pin grain growth at high temperatures, a novel steel chemistry was proposed in Part I of this work. The new composition results in a two phase ferrite/austenite microstructure which resists grain growth over a wide temperature range. The relationship between the austenite particle coarsening, the pinning force, and the kinetics of ferrite grain growth were established using samples that were reheated from room-temperature. In the present Fe-Al model steel, grain growth was inhibited up to 1578 K (1305 °C). All of the experiments performed in the companion paper involved reheating samples with a very homogenous microstructure and fine initial grain size. This differs from industrial TSCDR conditions where delta-ferrite and austenite grain growth both occur in the

TIHE ZHOU, Post-Doctoral Fellow, HATEM S. ZUROB, Associate Professor, and MANI SUBRAMANIAN, Professor, are with the Department of Materials Science and Engineering, McMaster University, 1280 Main Street, West Hamilton, ON L8S 4L7, Canada. Contact e-mail: zurobh@mcmaster.ca PENG ZHANG, Product Development Engineer, is with the Product Development, Essar Steel Algoma Inc., 105 West Street, Sault Ste. Marie, ON P6A 7B4, Canada. RONALD J. O'MALLEY, Professor, is with the, Department of Metallurgical Engineering, Missouri S&T, 284 McNutt Hall 1400 N. Bishop Ave., Rolla, MO 65409-0340.

Wt pct	C	Mn	Si	Al	Ti	Nb	N
Thin slab APIX70	0.05	1.60	0.30	0.025	0.012	0.07	0.008
APIX80	0.06	1.65	0.25	0.025	0.012	0.034	0.005
Fe-Al model alloy	0.051	1.00	0.36	1.5			

heterogeneous microstructure produced by solidification. The evolution of the volume fraction of pinning particles under reheating conditions is also very different from that expected under TSCDR conditions. In order to verify the effectiveness of the model alloy under industrial conditions it is necessary to simulate the TSCDR solidification process. In this contribution a laboratory-scale setup is developed to reproduce the as-cast microstructures and industrial cooling rates. The results are then analyzed using a physically-based model for grain growth. The possibility of using this new model alloy to control grain growth during TSCDR is also discussed.

II. MATERIALS AND EXPERIMENTAL PROCEDURE

A simple laboratory-scale setup was developed to simulate the microstructures obtained during the solidification and cooling of a steel made by the TSCDR process. The experiments consisted of melting a 30 kg heat of the model Fe-Al steel in an induction furnace under a controlled atmosphere (commercial purity Ar). A steel rod was briefly dipped into the molten metal to initiate solidification. The most important feature of this design is the possibility of interrupting solidification at a specific time by removing the rod from the liquid. The dipping bars were 80 mm long and had a diameter of 24.5 mm. Once the dipping bars were removed from the melt, the solidified shells were cooled down to room temperature at different rates using air, forced air, and water quenching. The cooling rate of each specimen was recorded using a B-type thermocouple and an acquisition frequency of 7.5 Hz. After the dipping tests, the furnace was turned off and the melt was allowed to solidify at a very slow cooling rate. The resulting ingot was vertical sectioned and samples were taken from the ingot surface to the center. For comparison, a 85 mm direct strip production complex (DSPC) slab of APIX70 (Chemistry listed in Table I) was sampled after solidification prior to entering the twin roller hearth tunnel furnaces at Essar Steel Algoma Inc. and was sectioned to measure the austenite grain size at various distances from the slab surface.

All the samples were prepared by using standard metallographic techniques. The delta-ferrite grain boundaries of the Fe-Al model steel were revealed using 2 pct Nital in ethanol. The prior austenite grain boundaries of APIX70 DSPC slab were revealed using a 200 mL aqueous solution of picric acid with 2 g sodium dodecylbenzene sulfonate wetting agent and 4 mL of hydrochloric acid.[6] The microstructure was studied using optical microscopy and scanning electron microscopy. Image analysis was performed using Clemex PE5.0 software. In order to obtain reliable statistics, at least six micrographs, containing at least 200 grains, were analyzed for each sample. In all cases, the grain size was measured using the linear intercept method and the true three-dimensional grain diameter was calculated as 1.61 times the linear intercept diameter.[7]

III. RESULTS

Figure 1 shows the microstructure evolution of model alloy shells that solidified on the steel bar that was dipped into the melt. Figure 1(a) corresponds to air cooling of the solidified shell down to room temperature, while Figures 1(b) and (c) correspond to forced-air and water cooling, respectively. The dark particles are the austenite phase which transformed to martensite and/or pearlite on cooling to room temperature and the matrix is delta-ferrite. The thermal profile that was measured during solidification in the above simulations is shown in Figure 1(d). In this experiment, the measured grain-growth kinetics is not isothermal and the complete thermal profile needs to be analyzed in order to quantitatively interpret the grain-growth data. A detailed description of this analysis is presented in the Section IV.

In addition, the ingot which resulted from the solidification of the model alloy melt within the furnace was analyzed. Six samples were obtained covering the microstructure from the surface to the centre of the ingot. The evolution of the grain-size as a function of position from the surface of the ingot is shown in Figure 2. The essentially constant grain-size as a function of depth suggests that the delta-ferrite grains were pinned by the austenite particles which are uniformly distributed within the ingot.

The microstructure of the industrially-cast, 85 mm, slab of APIX70 steel is shown in Figure 3. In contrast to the model Fe-Al steel, in which ferrite is always the dominant phase, the APIX70 steel is austenitic between ~1150 K and 1723 K (877 °C and 1450 °C). At the surface of the APIX70 slab, the (prior) austenite grain size is about 58 μm. At the centre of the slab, the (prior) austenite grain size is as large as 1342 μm. The industrial as-cast microstructure is non-uniform with extremely large grains at the centre.

IV. DISCUSSION

The use of the laboratory-scale setup described above permitted us to determine the microstructure evolution at different cooling rates. These cooling rates span the
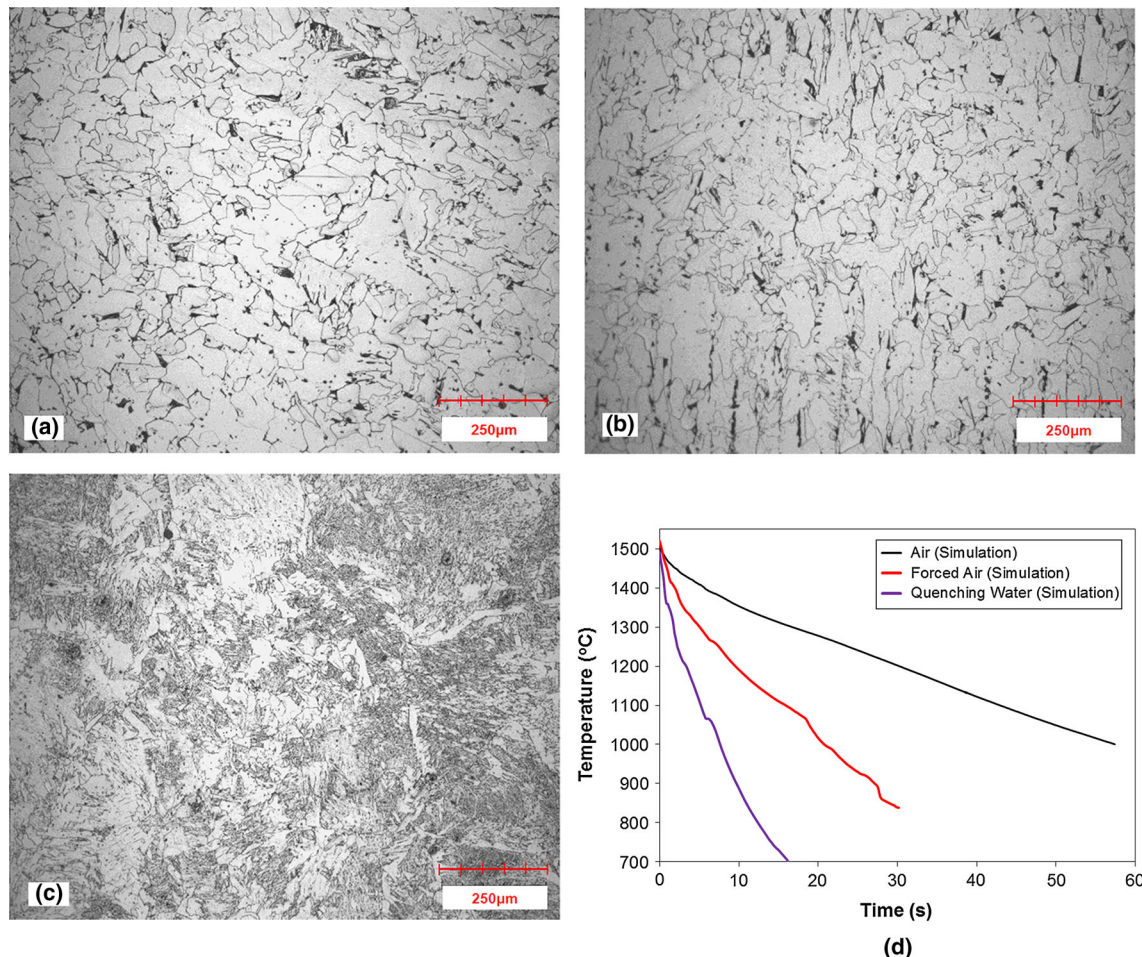
Fig. 1—Microstructure evolution of solidified shells of model Fe-Al alloy on a steel dipping bar with different cooling rates using (*a*) air, (*b*) forced air, (*c*) water quenching, and (*d*) the simulation thermal profile during solidification with different cooling rate.

range of cooling rates observed within an industrial thin slab. In this way, one can demonstrate the potential for grain-size control using the proposed model steel. To start the microstructure evolution during cooling is discussed in Section IV–A. The applications of this new alloy system to TSCDR, welding, and other applications requiring resistance to grain growth at high temperature is present in Section IV–B.

A. Experimental Validation: The Benefits of Fe-Al Model Alloy

Solidification starts when the dipping bar is submerged into the melt. Under equilibrium cooling conditions, the model Fe-Al steel will solidify as delta-ferrite and austenite precipitation occurs in the solid state at about 1583 K (1310 °C), as discussed in the companion paper. However, industrial cooling conditions will lead to non-equilibrium solidification and some austenite will form during solidification. Figures 1 and 2 confirm the presence of austenite precipitates along the delta-ferrite grain boundaries. In these figures the dark phase is austenite which transformed to pearlite or/and martens-

ite on cooling. The small grains along the grain boundaries may also correspond to austenite grains which transformed to ferrite during cooling to room temperature. Figure 4(a) is a magnified view of the solidified shell that was air cooled to room temperature. Figure 4(b) shows the grain size distribution for the same condition. The grain size exhibits a bi-modal distribution due to the transformation of some of the austenite particles to alpha-ferrite on cooling; the ferrite grains which formed from austenite during cooling are much finer than the delta-ferrite grains which formed during solidification

Using the assumption of no diffusion of the substitutional elements in the solid, the SCHEIL module of ThermoCalc[8] was used to analyze the phases formed during non-equilibrium cooling of the model steel. In this calculation, carbon back-diffusion in the solid is allowed to take place. As shown in Figure 5(a), the liquid will start to solidify as delta-ferrite at 1801 K (1528 °C). Once the temperature drops below 1728 K (1455 °C), the austenite phase will precipitate. The liquid, delta-ferrite, and austenite phases will coexist down to 1563 K (1290 °C). The predicted
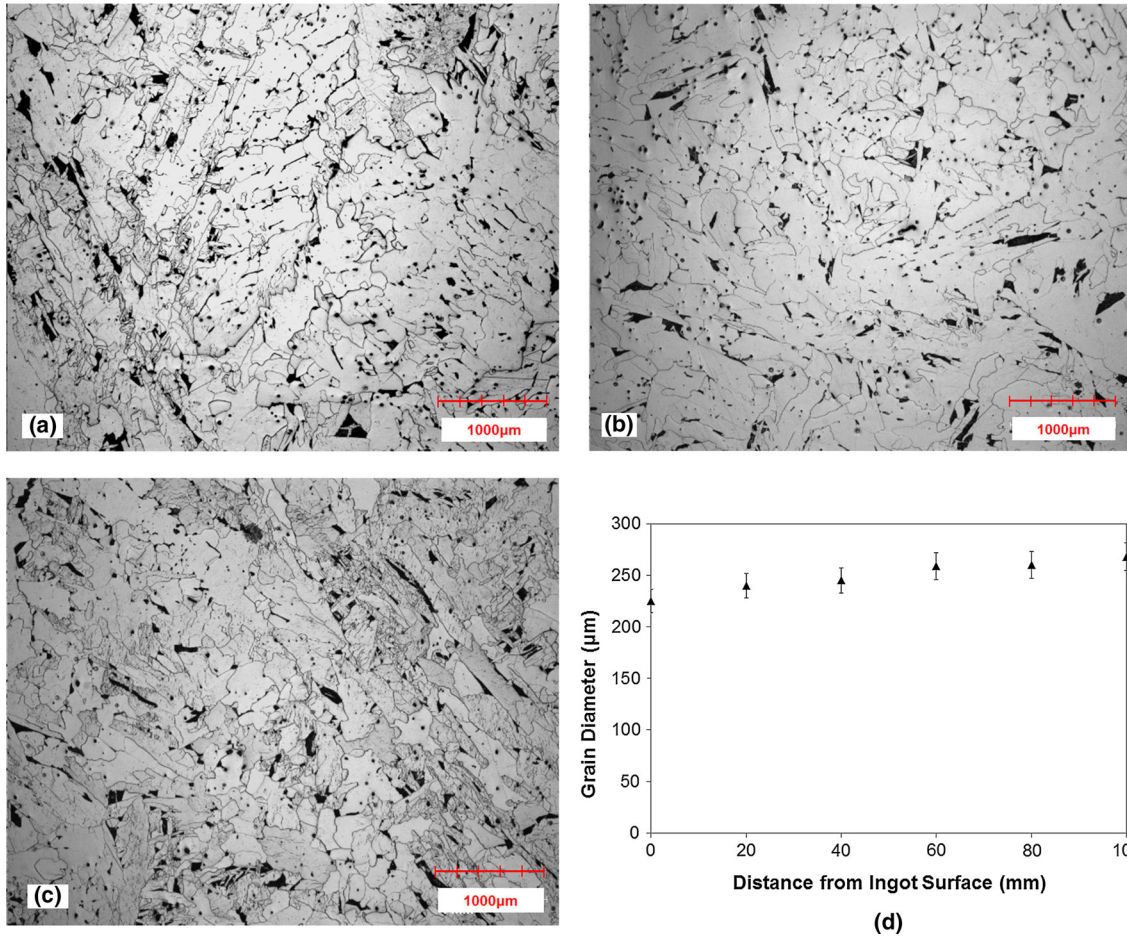
Fig. 2—Microstructure evolution of furnace cooled ingot of Fe-Al model alloy (a) close to ingot surface, (b) quarter way from ingot surface, (c) close to ingot center, and (d) summary of the measured delta-ferrite grain size with ingot distance from the ingot surface to center.

austenite mole fraction with temperature is shown is Figure 5(b). At 1718 K (1445 °C), the calculated volume fraction of austenite is about 0.5 pct. These particles are expected to form along the delta-ferrite grain boundaries as shown in Figures 1, 2, and 4(a). The austenite particles will exert a pinning pressure on the delta-ferrite grains and as the temperature decreases, the volume fractions of these particles will increase leading to complete pinning of the delta-ferrite grain growth.

In order to quantify the analysis, a simple non-isothermal grain-growth model[9] is utilized to capture the evolution of the delta-ferrite grain size in the Fe-Al model steel. Starting with the simple equation:

$$\frac{d\overline{R}}{dt} = \alpha M(t) \frac{2\gamma_{gb}}{\overline{R}}$$ [1]

and integrating with respect to time, leads to:

$$\overline{R}^2 = \overline{R}_o^2 + 4\gamma_{gb} \int_0^t \alpha M(t) dt,$$ [2]

where $\overline{R}$ is the mean radius of an individual delta-ferrite grain, $\overline{R}_o$ is the initial grain radius, which will be assumed to be 7.5 μm according to Figure 1(c), and γ_{gb} denotes the grain boundary energy per unit of area, a

reasonable value for which is 0.8 J m^{-2}.[10] Finally, $M(t)$ is the mobility of the delta-ferrite grain boundaries[9]*:

---

*In Ref.[9] the constant α was omitted from Eqs. [1] and [2]. As a result, the mobility calculated by Ref.[9] is actually the product $\alpha M(t)$.

$$\alpha M(t) = \frac{0.7075}{T(t)} \times \exp\left(\frac{-20995.43}{T(t)}\right).$$ [3]

In this equation $T(t)$ is an expression for the temperature as a function of time which was obtained experimentally from the data recorded, using a thermocouple, during solidification (Figure 1(d)).

The predicted delta-ferrite grain size, in the absence of pinning (solid line), is compared to the experimental data for the model Fe-Al steel for different cooling rates in Figure 6. The experimentally determined the delta-ferrite grain size was obtained from the mean of the second peak of the bimodal distribution shown in Figure 4(b) as this is believed to represent the original delta-ferrite grains present at high temperature. Evidently, the model over estimates the delta-ferrite grain size because particle pinning was not taken into account. In order to capture the effect of particle pinning, it is
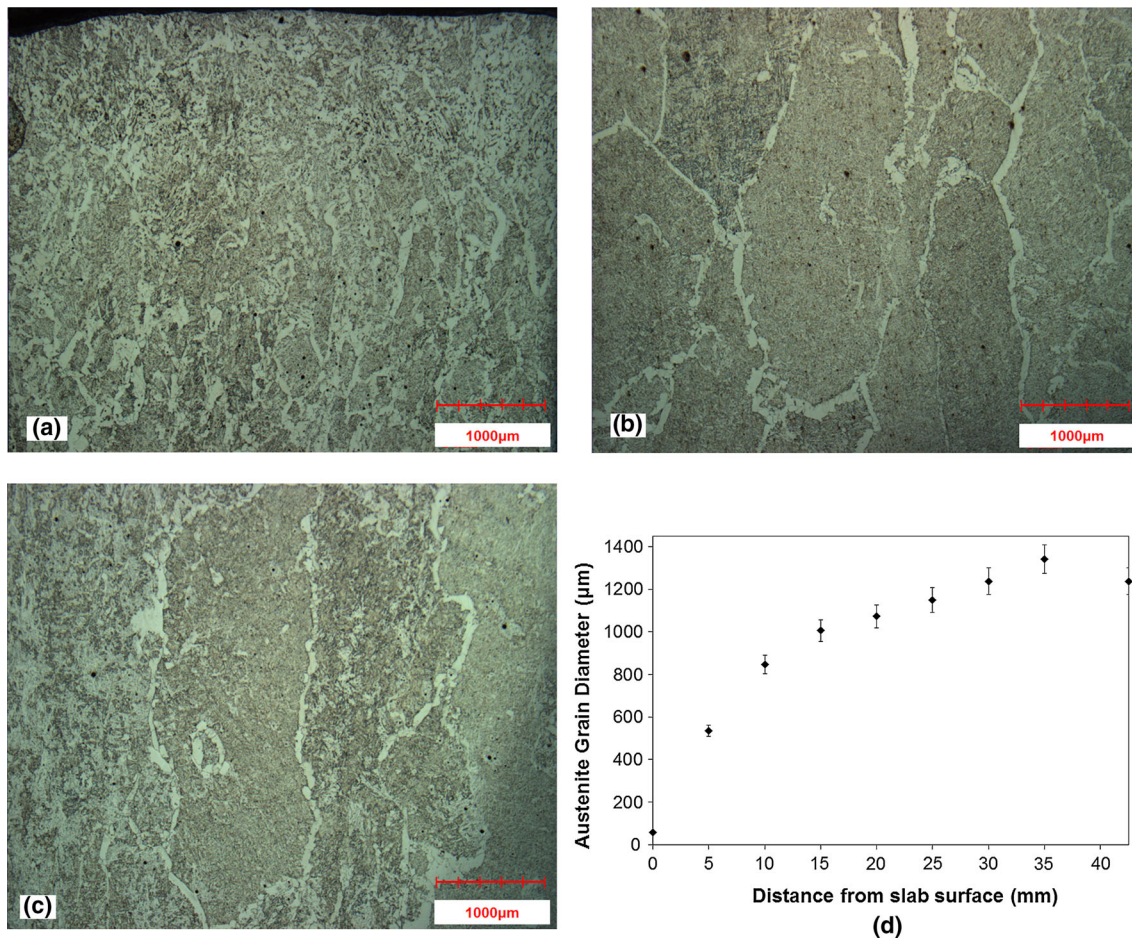
Fig. 3—85 mm slab austenite grain size evolution of DSPC practice APIX70 from industrial thin slab casting process (a) close to slab surface, (b) quarter way from slab surface, (c) close to the slab center, and (d) summary of the measured austenite grain size with distance from slab surface to center.

assumed that the delta-ferrite grains are completely pinned by the austenite particles as soon as the austenite phase appears. The temperature at which the austenite forms was estimated from the Scheil model and the predicted delta-ferrite grain-size evolution was plotted as the dot–dash curves in Figure 6. The very good agreement between the model predictions, in the presence of pinning, and the experimental data confirms the effectiveness of model alloy in inhibiting high temperature grain growth under post-solidification cooling conditions.

It is interesting to note that in spite of the wide range of cooling rates that were investigated in the dipping tests, the resulting delta-ferrite grain size varied over a narrow range (~200 μm for air cooling and 90 μm for water cooling). Even under the extremely slow cooling rates obtained by furnace cooling the model Fe-Al steel ingot, the grain size did not exceed 275 μm. The behavior of the model alloy stands in sharp contrast to the industrially cast APIX70 slab in which a large variation of grain size was observed as shown in Figure 3. In particular, the model alloy did not have any excessively large grains similar to those found at the center of the APIX70 slab. The efficient grain size control in the model steel is attributed to the pinning

pressure that the austenite particles exert on the delta-ferrite grains. The smaller grain size and more uniform microstructure of the model alloy provides a better starting point for thermomechanical processing compared to heterogeneous microstructure of APIX70.

B. Applications

The model Fe-Al steel exhibited grain pinning at high temperature during reheating (discussed in Paper 1) and during solidification (validated in Section IV–A). This could have potential applications in the area of TSCDR process to produce fine and uniform as-cast microstructure. The present approach may also find applications in the area of grain size control in the heat affected zone (HAZ) of welds and for the development of materials with excellent resistance to grain growth at high temperatures.

1. Application to thin slab casting direct rolling process

During TSCDR process grain growth occurs during the cooling of the solidified slab as well as isothermal holding in the soaking furnace. Figure 7(a) shows the temperature profile at the surface as well as those at 5 and 10 mm below the surface of an 85 mm, APIX70
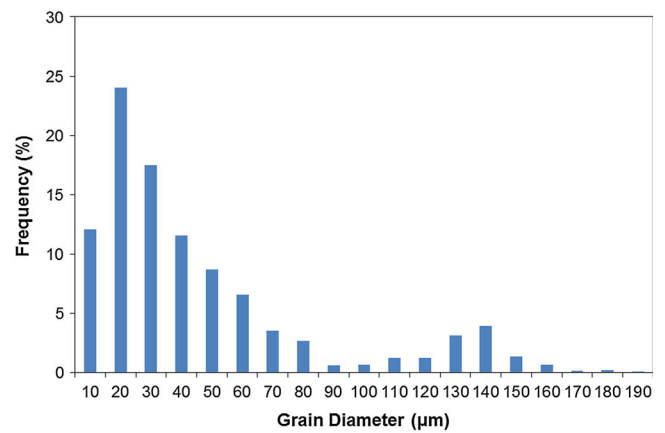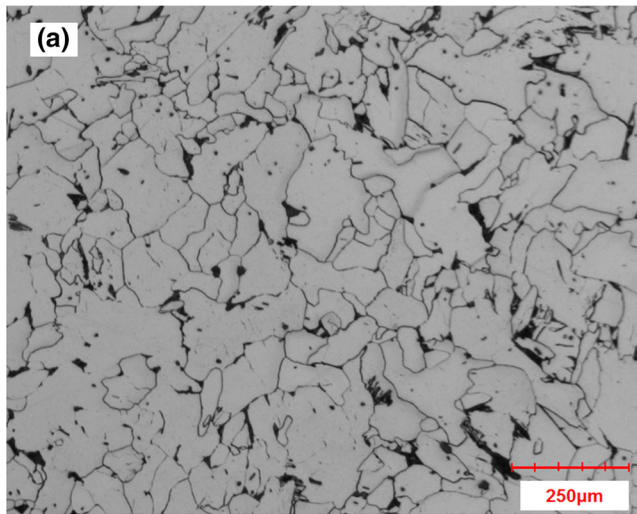
Fig. 4—(a) Microstructures of Fe-Al model alloy using steel the steel dipping bar cooling down in air. (b) Grain size distribution of Fe-Al model alloy using steel dipping bar using air cooling.
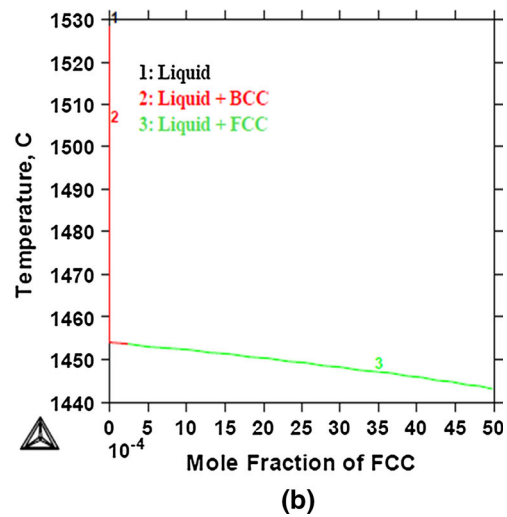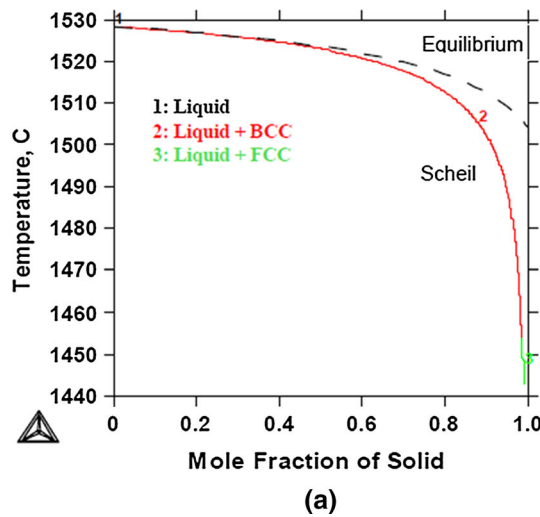

Fig. 5—ThermoCalc using SCHEIL model predicted non-equilibrium solidification. (a) Mole fraction of solid, (b) mole fraction of austenite particle.

slab, cast at a speed of 3.4 m/min at Essar Steel Algoma Inc. using the DSPC process. The temperature profiles are calculated using the CON1D slab casting heat transfer model.[11] The figure also includes the recorded thermal profile obtained from the laboratory solidification experiments using the model alloy. The simulated cooling rate, using water quenching, was 108 K/s [averaged value between 1773 K and 1523 K (1500 °C and 1250 °C)], which is similar to the cooling rates observed on the slab surface ($\dot{T}$ = 106 K/s). The forced-air cooling rate, $\dot{T}$ = 33 K/s, and the static air cooling rate, $\dot{T}$ = 10.5 K/s, are close to the cooling rates predicted at 5 mm (average rate of 9 K/s) and 10 mm (average rate of 8.3 K/s) below the surface of the industrially cast 85 mm slab. One can therefore compare the average grain sizes obtained from the dipping tests to the grain-sizes measured at 0, 5, and 10 mm below the surface of the industrial slab. In addition, the cooling

rate for the furnace cooled Fe-Al steel ingot was extremely slow and could be compared to that at the center of the industrially cast slab. These comparisons are shown in Figure 7(b), in which, the grain-size prior to entry into the soaking furnace was obtained by directly measuring the prior austenite grain size as a function of distance from the surface of the slab (Figure 3(d)). The data points for the model steel were positioned by matching the cooling rates in the dipping test to the position at which these cooling rates would be observed within the slab. Based on this comparison, if the model steel was cast in the form of an 85 mm slab, the expected grain size at the center would be 280 μm, compared to 1340 μm for APIX70. This clearly demonstrates the potential advantage of the model alloy. One could also compare the grain-sizes within the APIX70 slab after exiting the soaking furnace, to those expected in the model alloy. To perform this comparison the
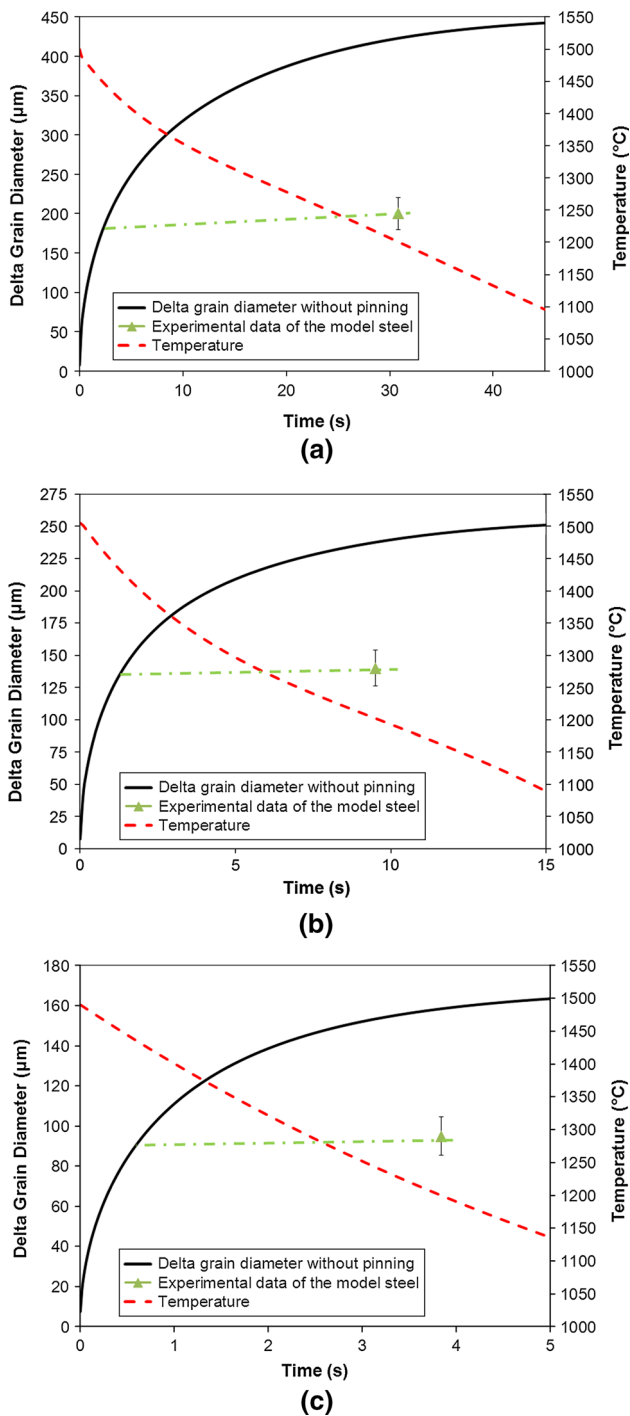
Fig. 6—Comparison of the predicted delta grain size without pinning and experimental data (with pinning) with different cooling rates (*a*) air. Comparison of the predicted ferrite grain size without pinning and experimental data (with pinning) with different cooling rates (*b*) forced air. Comparison of the predicted delta grain size without pinning and experimental data (with pinning) with different cooling rates (*c*) water quenching.

experimentally measured grain sizes within the APIX70 slab prior to entering the soaking furnace were used as the initial values in Eq. [2] and the grain size after 18 minutes of holding at 1423 K (1150 °C) was calcu-

lated and plotted in Figure 7(b). The use of Eq. [2], which does not include pinning, is justified based on prior work[9] which demonstrated that the TiN particles formed in this steel exerted a small pinning effect during soaking. In contrast, minimal grain growth is expected in the model steel as a result of the strong pinning exerted by the austenite particles. As a result, the grain size of the model alloy is essentially unchanged as a result of soaking.

Figure 7(b) shows that, prior to entering the soaking furnace, the austenite grain-size in APIX70 is non-uniform with finer grains being present near the surface. After homogenization, the grains at the surface grow significantly reaching a size of 600 μm, while the large grains at the center reach a size of almost 1500 μm. The results clearly show the advantage of the proposed model alloy. In contrast, the model Fe-Al steel can prevent excessive grain growth prior to the onset of thermomechanical processing. The grain-size distribution obtained using the model alloy provides a much better starting point for thermomechanical processing, compared to that obtained using APIX70. One should keep in mind, however, that ferrite is the predominant phase at all temperatures in the model steel. As a result, no additional grain refinement can be obtained as a result of phase transformations during cooling. In contrast, the APIX70 steel, which is austenitic in the hot rolling temperature range, will experience grain refinement during cooling due to the austenite to ferrite phase transformation. A complete analysis that considers grain growth, thermomechanical processing, and phase transformations is therefore needed to determine the actual benefit of using the proposed Fe-Al model steel. Another important aspect that needs to be considered is the effect of austenite on the homogenization of the as-cast microstructure. It is generally desired that the steel solidify as single-phase delta-ferrite in order to avoid solute partitioning between austenite and ferrite and in order to take advantage of the fast diffusion of substitutional elements in delta-ferrite to reduce microsegregation. Further investigation is needed to confirm that the formation of a small volume fraction of austenite at the late stages of solidification will not have a negative impact on the homogeneity of substitutional elements in the steel.

2. Application to welding process

During welding, the base metal lying adjacent to the fused zone will be subjected to one or more high temperature thermal cycles. These thermal cycles will introduce significant changes in the microstructure and mechanical properties within the HAZ. Weld strength is a dominating factor in assessing the overall performance of steels for the manufacturing of pipelines, tubing, and casings. Large austenite grains near the fusion line may promote the formation of martensitic or bainitic transformation products with adverse effects on weld properties.[12–14] In conventional low alloy steels, the fine niobium, titanium, or vanadium carbonitrides that inhibit austenite grain growth will dissolve or coarsen within the HAZ. As a result, excessively large austenite
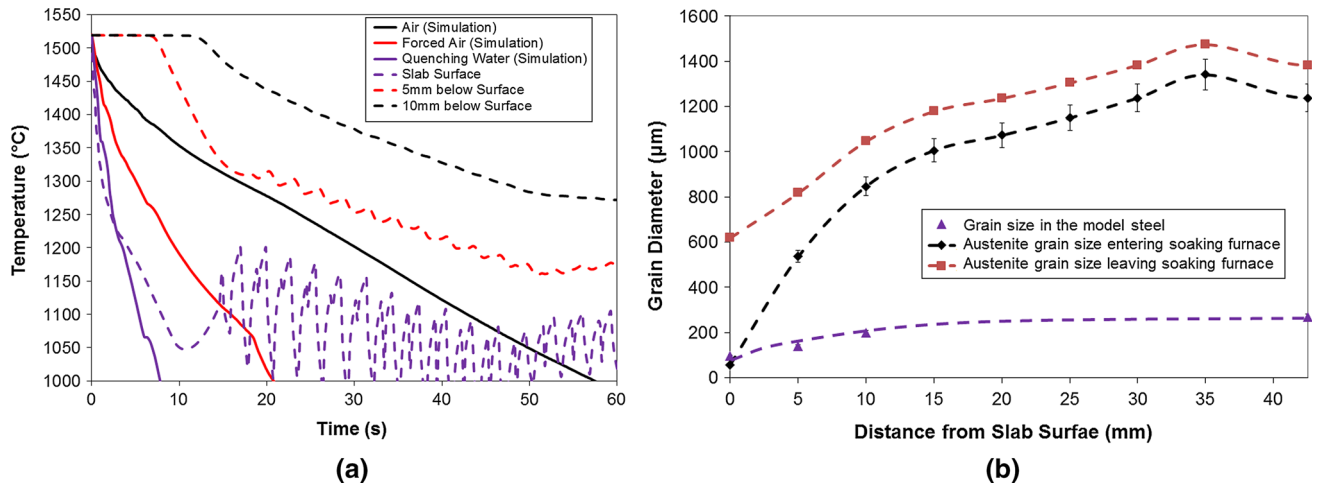
Fig. 7—(a) Comparison of CON1D predicted temperature profiles on the surface, 5 and 10 mm below the APIX70 85 mm slab and the recorded thermal profile during simulation process. (b) Comparison of grain size evolution with slab distance using TSCDR process to produce APIX70 and Fe-Al pct model alloy.
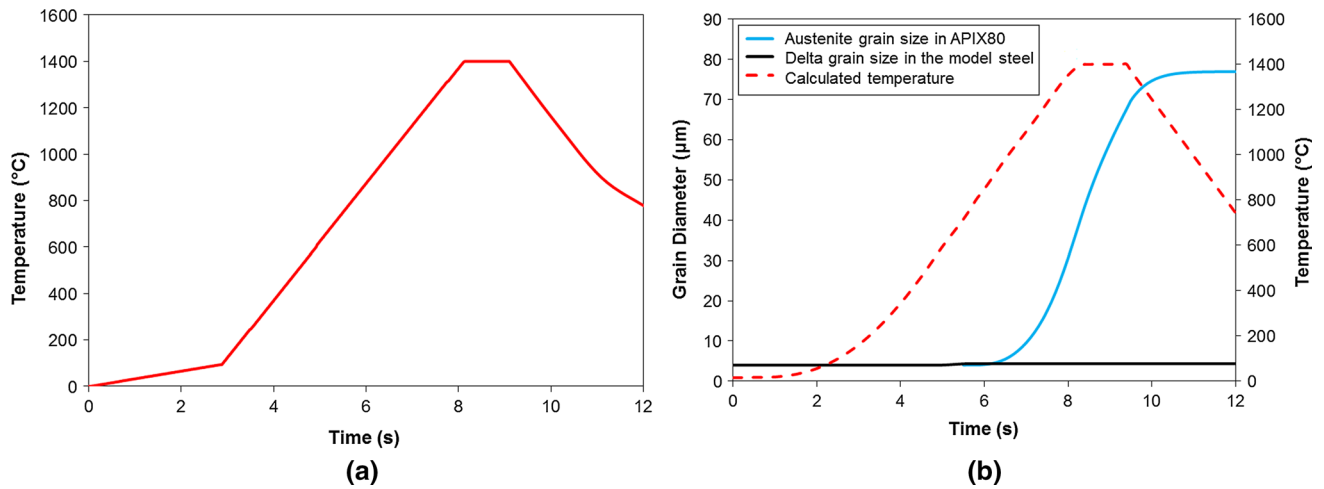

Fig. 8—(a) A heating profile for APIX80 during a welding trial[17]. (b) Comparison of model predicted austenite grain size in APIX80 and delta grain size in model Fe-Al alloy during welding process.

grains may develop within the HAZ. The proposed model Fe-Al steel can prevent austenite coarsening in the HAZ. Figure 8(a) shows the heating profile measured during the welding of an APIX80 steel, whose chemistry is shown in Table I.[15] The steel was heated at a rate of 250 K/s to a peak temperature of 1673 K (1400 °C) followed by cooling at 250 K/s. In order to model grain growth during this heating cycle, the microalloyed APIX80 steel was assumed transforms to austenite at 993 K (720 °C). The austenite grain-growth was modeled by integrating Eq. [2] from t_1 to t, where t_1 is the time corresponding to the completion of the alpha-ferrite/pearlite to austenite phase transformation during heating. The product of α and austenite grain boundaries mobility is 0.3 times of Turnbull estimate[9,16,17]:

$$\alpha M(t) = \frac{0.1920}{T(t)} \times \exp\left(\frac{-20837.14}{T(t)}\right), \qquad [4]$$

where $T(t)$ is obtained from the heating profile of Figure 8(a). The calculated grain-size evolution for APIX80 is shown in Figure 8(b). An initial austenite grain-size of 4 μm was assumed in the above calculation. For comparison, the ferrite grain size in the model alloy is not expected to change during the above heating cycle due to the strong pinning effect exerted by the austenite particles. A critical assumption here is that the short time (~2 seconds) spent above the austenite dissolution temperature 1578 K (1305 °C) would not lead to the complete dissolution of the austenite particles and unpinning of the delta-ferrite grains. The vulnerability of the alloy for excessive grain growth above 1578 K (1305 °C) could
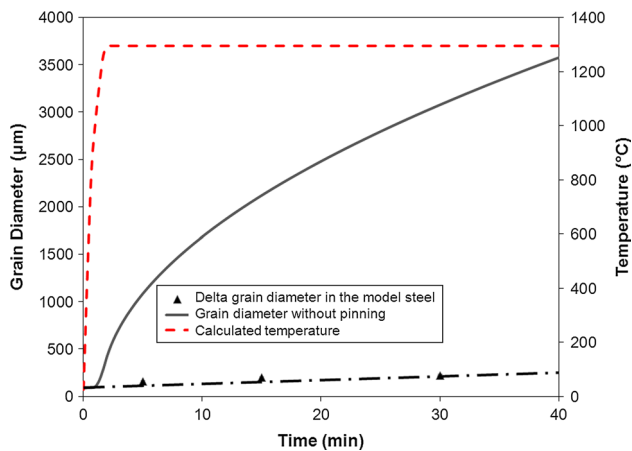
Fig. 9—Comparison of model predicted delta grain growth without particle pinning and experimented measurement of delta-ferrite grain diameter in model Fe-Al steel at 1568 K (1295 °C).

be addressed by changing the Al content in order to increase the austenite dissolution temperature.

3. *Steel that resists grain growth at high temperature*

As discussed in the companion paper, the delta-ferrite grain growth in the model steel is dominated by the pinning effect of the austenite particles. At high temperature the delta-ferrite grains grow at a rate which is controlled by rate of coarsening of the austenite particles. As a result, the growth of the delta-ferrite grains occurs at a very slow rate due to the fact that austenite particles are large (micron scale) and consequently have a small diving force for coarsening. Thus, the proposed new alloy is a promising candidate for high temperature applications which require stable grain size. In Figure 9, the experimental grain growth kinetics in this two phase material is compared with the predicted grain-growth kinetics in the absence of pinning 1568 K (1295 °C). The temperature profile, shown on the secondary axis, was obtained experimentally form the data recorded by the thermocouple attached to the specimen (please refer to companion paper). The solid points refer to the delta-ferrite grain diameter which was experimentally measured in the model Fe-Al alloy. For comparison, the ferrite grain-size in the absence of particle pinning was calculated using Eq. [2] and the ferrite grain boundary mobility.[9] When these two materials are heated to 1568 K (1295 °C) for 5 minutes, the materials without particle pinning is predicted to have a grain size of 1100 μm, while, the model alloy is expect to have a grain size of 157 μm.

V. CONCLUSIONS

1. Solidification and cooling rate simulations confirmed that the proposed Fe-Al model alloy can resist grain growth under industrial solidification and cooling conditions. During non-equilibrium solidification, the austenite phase precipitates along the delta-ferrite grain boundaries. The austenite particles pin the delta-ferrite grain growth during cooling and soaking. As a result, a finer and more uniform as-cast macrostructure can be obtained.

2. The proposed austenite/ferrite two phase alloy has the potential to control grain size and prevent excessive grain growth during the process of TSCDR. During welding, the novel alloy can greatly limit coarsening in the HAZ. More generally, this material can be used to prevent grain growth at high temperature due to the presence of a stable distribution of pinning particles.

REFERENCES

1. C. Klinkenberg, C. Bilgen, J.M. Rodriguez-Ibabe, B. Lopez, and P. Uranga: *Mater. Sci. Forum*, 2012, vols. 706–709, pp. 2752–57.
2. G. Arvedi, F. Mazzolari, J. Siegl, G. Hohenbichler, and G. Holleis: *Ironmak. Steelmak.*, 2010, vol. 37 (4), pp. 271–75.
3. K. Hensger, L. Leduc Lezama, and F. Siciliano: *33rd McMaster Symposium on Iron & Steelmaking: Thinner Slab Casting*, G.A. Irons, ed., McMaster University, Hamilton, 2005, pp. 262–76.
4. S.J. Cobo and C.M. Sellars: *Ironmak. Steelmak.*, 2001, vol. 28 (3), pp. 230–36.
5. P. Uranga, A.I. Fernández, B. López, and J.M. Rodriguez-Ibabe: *Mater. Sci. Forum*, 2005, vols. 500–501, pp. 245–52.
6. N.S. Pottore, C.I. Garcia, and A.J. DeArdo: *Metall. Trans. A*, 1991, vol. 22A, pp. 1871–80.
7. T. Gladman: *The Physical Metallurgy of Microalloyed Steel*, Institute of Materials, London, 1997, pp. 159–161.
8. Available from Thermo-calc Software: www.thermocalc.com. Accessed 7 Oct 2014.
9. T. Zhou, R.J. O'Malley, and H.S. Zurob: *Metall. Mater. Trans. A*, 2010, vol. 41A, pp. 2112–20.
10. J.W. Martin, R.D. Doherty, and B. Cantor: *Stability of Microstructure in Metallic System*, Cambridge University Press, Cambridge, 1997, pp. 219–31.
11. Y. Meng and B.G. Thomas: *Metall. Mater. Trans. B*, 2003, vol. 34B, pp. 685–705.
12. L.P. Zhang, C.L. Davis, and M. Strangwood: *Metall. Mater. Trans. A*, 1999, vol. 30A, pp. 2089–96.
13. F. Hamad, L. Collins, and R. Volkers: *Proc. 7th Int. Pipeline Conf. (IPC2008)*, ASME, Calgary, 2008, IPC2008-64097.
14. R.A. Silva, G.Z. Batista, L.F.G. de Souza, and I.S. Bott: *Mater. Sci. Forum*, 2012, vols. 706–709, pp. 2059–65.
15. K. Banerjee, M. Militzer, M. Perez, and X. Wang: *Metall. Mater. Trans. A*, 2010, vol. 41A, pp. 3161–72.
16. D. Turnbull: *Trans. AIME*, 1951, vol. 191, pp. 661–65.
17. T. Zhou and H.S. Zurob: *Can. Metall. Q.*, 2011, vol. 50 (4), pp. 389–95.